MOLECULAR AND CELLULAR BIOLOGY, Feb. 2007, p. 1069–1082 Vol. 27, No. 3
0270-7306/07/$08.00+0 doi:10.1128/MCB.01674-06
Copyright © 2007, American Society for Microbiology. All Rights Reserved.

Individual Subunits of the Ssn6-Tup11/12 Corepressor Are Selectively Required for Repression of Different Target Genes▽†

Fredrik Fagerström-Billai,* Mikaël Durand-Dubief, Karl Ekwall, and Anthony P. H. Wright

School of Life Sciences, Södertörns Högskola, SE-141 89 Huddinge, and Department of Biosciences and Nutrition, Karolinska Institutet, SE-141 57 Huddinge, Sweden

Received 7 September 2006/Returned for modification 2 October 2006/Accepted 5 November 2006

The *Saccharomyces cerevisiae* Ssn6 and Tup1 proteins form a corepressor complex that is recruited to target genes by DNA-bound repressor proteins. Repression occurs via several mechanisms, including interaction with hypoacetylated N termini of histones, recruitment of histone deacetylases (HDACs), and interactions with the RNA polymerase II holoenzyme. The distantly related fission yeast, *Schizosaccharomyces pombe*, has two partially redundant Tup1-like proteins that are dispensable during normal growth. In contrast, we show that Ssn6 is an essential protein in *S. pombe*, suggesting a function that is independent of Tup11 and Tup12. Consistently, the group of genes that requires Ssn6 for their regulation overlaps but is distinct from the group of genes that depend on Tup11 or Tup12. Global chip-on-chip analysis shows that Ssn6 is almost invariably found in the same genomic locations as Tup11 and/or Tup12. All three corepressor subunits are generally bound to genes that are selectively regulated by Ssn6 or Tup11/12, and thus, the subunit specificity is probably manifested in the context of a corepressor complex containing all three subunits. The corepressor binds to both the intergenic and coding regions of genes, but differential localization of the corepressor within genes does not appear to account for the selective dependence of target genes on the Ssn6 or Tup11/12 subunits. Ssn6, Tup11, and Tup12 are preferentially found at genomic locations at which histones are deacetylated, primarily by the Clr6 class I HDAC. Clr6 is also important for the repression of corepressor target genes. Interestingly, a subset of corepressor target genes, including direct target genes affected by Ssn6 overexpression, is associated with the function of class II (Clr3) and III (Hst4 and Sir2) HDACs.

Gene regulation by corepressors is an important mechanism for controlling the transcriptional activity of the genome. The global yeast Ssn6/Tup corepressor, mainly characterized in *Saccharomyces cerevisiae*, is conserved in all fungi and has functional homologues in higher eukaryotes, such as Groucho and TLE (26, 43). The multifunctional Ssn6/Tup corepressor is recruited to target genes by interactions with DNA-binding repressor proteins and regulates a wide variety of processes, such as glucose utilization (33), mating type (25), DNA damage repair (20), and stress response (37). The Tup1 protein consists of a highly conserved WD 40 repeat domain which is believed to be important for interaction with other proteins via a propeller-like ring structure (36, 56). The Tup1 tetramer is thought to interact with the N terminus of the Ssn6 protein to form a corepressor complex (14, 23, 48). In the fission yeast, *Schizosaccharomyces pombe*, there are two paralogous *TUP1*-like genes encoding the Tup11 and Tup12 proteins (18, 24, 32). Tup11 and Tup12 have some redundant functions (18, 24), but there is also a clear difference in the roles of Tup11 and Tup12 in stress responses (13). Tup11 and Tup12 can interact with each other and with the *S. pombe* Ssn6 protein (13), but it is not clear whether they coexist in individual corepressor complexes or whether they participate in distinct corepressor pools that are recruited to overlapping but distinct sets of genes.

The Ssn6 protein is characterized by a central 10-copy tetratricopeptide repeat domain, which provides a protein interaction surface that mediates the interaction with Tup1 (41, 43) as well as recruitment of the complex to target genes by different DNA-bound repressor proteins (26, 47). The different tetratricopeptide repeat motifs play an important role in the specificity of Ssn6 interaction with different repressor proteins (44, 46). Ssn6 can form functional complexes with mammalian Tup1 homologues, such as TLE, suggesting involvement of mammalian Ssn6-like proteins in repressor complexes in mammals that are analogous to those found in fungi (17). The closest human Ssn6 homologues are encoded by the ubiquitously transcribed Y and X chromosome genes, UTY and UTX, which are involved in dosage compensation and X/Y chromosome inactivation (30).

It has been suggested that the Tup1 tetramer is the major contributor to the repression activity of the complex (26, 47, 56). The similarity between the expression profiles of *TUP1*Δ and *SSN6*Δ strains (21) is consistent with a role of Ssn6 as a bridging protein between DNA-bound repressor proteins, which define target genes, and Tup1, which represses their activity. The repression activity of the Ssn6/Tup1 corepressor appears to be dependent on several different mechanisms that contribute independently (57). First, Ssn6/Tup1 repression is linked to chromatin modifications, and Tup1 has been shown to bind hypoacetylated histone H3 and H4 N-terminal tails directly (11, 12). Second, Ssn6/Tup1 interacts physically with class I and II histone deacetylases in *S. cerevisiae*, and the localization of Tup1 has been correlated to decreased acetylation levels in the subtelomeric regions of chromosomes (9, 50, 52). As a result of these or as yet undiscovered mechanisms,

* Corresponding author. Mailing address: School of Life Sciences, Södertörns Högskola, SE-141 89 Huddinge, Sweden. Phone: 46 8 6084714. Fax: 46 8 6084510. E-mail: fredrik.fagerstrom@sh.se.

† Supplemental material for this article may be found at http://mcb.asm.org/.

▽ Published ahead of print on 13 November 2006.

TABLE 1. *S. pombe* strains used in this study

Strain	Genotype	Reference or source
JY741	*ura4-D18 leu1-32 ade6M216*	32
tup11Δ tup12Δ	*Δtup11::ura4$^+$ Δtup12::leu2$^+$ h$^-$ ura4-D18 leu1-32 ade6M216*	32
FFB010	*ssn6::kanMX//ssn6$^+$ h$^-$ ura4-D18 leu1-32 ade6M210*	This study
Hu497	*ssn6GFP kanMX h$^+$ ura4-D18 leu1-32 ade6-210*	13
Hu853	*tup11GFP kanMX h$^+$ ura4-D18 leu1-32 ade6M210*	13
Hu851	*tup12GFP kanMX h$^+$ ura4-D18 leu1-32 ade6-M210*	13
Hu494	*ssn6HA-ts kanMX h$^+$ ura4-D18 leu1-32 ade6-210*	13
LPY3277	*Δhst4::his3$^+$ h$^-$ ura4-D18 leu1-32 ade6M216 his3-D1 arg3-D4*	15

Ssn6/Tup1 has also been shown to influence the organization of nucleosomes at target promoters (8). A third mechanism of repression by Ssn6/Tup1 is direct interference with the polymerase II transcriptional machinery (54). Several subunits of RNA polymerase II and the mediator subcomplex have been identified in genetic screens for mutants that are unresponsive to Tup1 (19, 38). Some of these components, such as the Hrs1/Med3 and Srb10 subunits of the mediator, interact directly with the corepressor (29, 34). Interestingly, Ssn6/Tup1 appears to play a role in the derepression of genes together with the SAGA and SWI/SNF complexes (7, 35, 37, 45). Furthermore, Ssn6 has recently been identified as a coactivator involved in the Gcn4-dependent activation of multiple gene targets (27).

In this study we have investigated the role of Ssn6 in *S. pombe* and its relationship to the function of the Tup11 and Tup12 proteins. The results show that (i) Ssn6 and the Tup11/12 proteins are required for regulation of distinct but overlapping groups of genes, consistent with the different phenotypes associated with defects in Ssn6 and Tup11/12; (ii) localization of all three corepressor subunits is highly correlated at both common and selective targets of Ssn6 and Tup11/12, consistent with the existence of a single predominant form of the corepressor complex containing all three subunits; (iii) the corepressor is preferentially associated with intergenic regions as expected but is also found in the coding regions of many genes; and (iv) the class I histone deacetylase (HDAC), Clr6, is the major HDAC responsible for deacetylation and repression of corepressor target genes, but Clr3 (class II) and Hst4 (class III) also play an important role at some corepressor target genes.

MATERIALS AND METHODS

Strains. The *S. pombe* strains in this study are listed in Table 1. LPY3277 encodes a defective Hst4 protein lacking residues 75 to 162. The *ssn6$^+$* open reading frame (ORF) was deleted by a PCR strategy described previously (3). The following primer pairs were used for generation of a KanMX cassette from the pFA6 plasmid for deletion of *ssn6$^+$*: 5′-TTCCCGCGTATCAGCT ACACCAGTATCATCAATTTTTAAAATATGTATGACTATTGTAAGCA AATTTCAAATGTGAGCGAATTCGAGCTCGTTTAAAC-3′ and 5′GTG GTTTACGTGGATTTCGTTCTCTGAACTTTTCCTTTTCCATAAGCGG ATGTTGCATTCTTGAAGAATTTCTATTCTCGGATCCCCGGGTTAAT TAA-3′. Amplified fragments were transformed into the wild-type diploid HU118 strain via electroporation, and correct insertion was confirmed by Southern blotting and PCR. Strains were cultivated at 30°C in rich yeast extract medium YES, containing 0.5% yeast extract and 3% glucose and supplemented with 75 mg required amino acids per liter media or in minimal media MM described previously (1). Kanamycin (200 mg/liter) was added to rich media 75, and 5-flouroorotic acid (5-FOA, 0.1%) was added to MM-uracil media after autoclaving. All extractions for immunoprecipitation and microarray analysis were made from cells grown in rich media except where selection for plasmids was appropriate (13).

Immunofluorescence microscopy. An endogenously tagged Ssn6GFP strain was grown for 18 h to mid log phase (1×10^7 cells/ml), harvested, fixed with formaldehyde, and incubated with primary anti-green fluorescent protein (anti-GFP, polyclonal rabbit 11121; Molecular Probes) and secondary antibodies (fluorescein isothiocyanate conjugated; Jackson Immunoresearch Laboratories) as described previously (4). Nuclear staining was performed with 4′,6′-diamidino-2-phenylindole (DAPI). The cells were subjected to fluorescence microscopy using a Zeiss Axioscope II microscope. Images were captured and analyzed using the Openlab software by Improvision.

Microarray analysis. RNA was extracted from cells as described in reference 53, except that the *ssn6HA-ts* strain was shifted to 36°C for 1 h before extraction of RNA and the Ssn6-overexpressing cells were grown in MM-uracil medium at 30°C. Two RNA samples from independent cultures were prepared for each condition, and 25 μg of RNA was subjected to reverse transcription (11904-018; Invitrogen) and labeled with CY3 (CY3 dCTP 53021; Amersham) or CY5 (CY5 dCTP 55021; Amersham) prior to hybridization on *S. pombe* gene microarrays from Eurogentec SA, Belgium (53). Altogether, four data points were generated for each condition and gene using two microarrays spotted in duplicate with two independent biological samples labeled in dye swap. The microarray signals were measured using a Scanexpress laser scanner and quantified using the Spotfinder quantification software (TIGR). The data were normalized using the Lowess per spot per chip method, analyzed, and filtered using Genespring software (Silicon Genetics). For microarray datasets and generated gene lists, see NCBI GEO submissions (http://www.ncbi.nlm.nih.gov/geo/), accession number GSE4566, and the supplemental material.

RT-PCR. RNA was extracted as described above and subjected to DNase treatment and reverse transcription (RT, 11904-018; Invitrogen) for synthesis of cDNA. Samples were subjected to PCR analysis in real time with SYBR green quantification. Enrichment relative to the wild type (WT) and *actin$^+$* expression levels was calculated with results from triplicate samples.

Chromatin immunoprecipitations. Chromatin immunoprecipitations were essentially performed as described previously (39, 51). Cells were grown to mid log phase (1×10^7cells/ml) in rich YES media. All cells were harvested at room temperature and immediately subjected to cross-linking with 10 mM dimethyl adipimidate and 0.25% dimethyl sulfoxide for 45 min, followed by 1% formaldehyde treatment for 2 h. Cross-linking was stopped for 15 min with 2.5 M glycine, and cells were washed in phosphate-buffered saline and lysed in a fast prep bead beater with lysis buffer (150 mM NaCl) and protease inhibitors. The lysate was subjected to sonication three times for 60 s for generation of chromatin fragments with an average length of 1 kb. The lysate was removed by centrifugation for 10 min at 13,000 rpm, and cell debris was sonicated for a further 60 s. The clear cell lysate from the two sonications was pooled, aliquoted, and subjected to immunoprecipitation with a polyclonal anti-GFP antibody 1:100 (8372-2; Applied Biosciences) and protein A Sepharose beads (17-5280-01; Amersham). Chromatin-bound beads were washed with 2× lysis buffer (500 mM NaCl) and with 2× deoxycholate buffer (0.1% sodium dodecyl sulfate) and eluted from beads with *N*-tris(hydroxymethyl)methyl-2-aminoethanesulfonic acid (TES, 1.5% sodium dodecyl sulfate) buffer. Cross-linking was reversed overnight at 65°C, and samples were treated with protease K and glycogen for 2 h at 57°C. DNA was purified by phenol-chloroform extraction and ethanol-sodium acetate precipitation. Input (1:200) and precipitates were subjected to SYBR green quantification with real-time PCR using primers specific for intergenic regions (IGR). Binding ratios were calculated as the difference in the precipitated fraction from input DNA as Input-IP(AB)/Input-IP(NOAB) relative to the binding to a control (tRNA glutamyl synthetase) IGR. The average values were derived from triplicate samples from independent ChiP experiments and calculated along with the standard error of the mean.

Genome-wide chromatin binding maps. Precipitated chromatin and input DNA fragments from three independent experiments were subjected to a two-step linear amplification as described previously (51). Round A was performed with Sequenase (USB 70775Y) and TPCRA priming. Round B was performed with Amplitaq (Roche) with TPCRB priming. Amplified material (500 to 1,000 ng) was subjected to Klenow labeling (18094-011; Invitrogen) with Cy3 and Cy5 (53021 and 55021; Amersham). Input fragments were labeled with Cy3, and

precipitated material was labeled with Cy5. Labeled fragments were hybridized to IGR plus ORF microarrays from Eurogentech SA, Seraing, Belgium (51). Microarray signals were measured using a ScanExpress laser scanner and quantified with the Spotfinder quantification software (TIGR). Data were analyzed and median normalized to the 50th percentile using GeneSpring software (Silicon Genetics) to generate six data points for each binding map. Flagged values were removed from the data set, and ratios were subjected to median percentile ranking analysis described previously (5). Median rank values were calculated with both combined IGR and ORF values and with separate individual ORF and IGR values. Cutoff values for the generation of binding lists were set to the 85th percentile. For chromatin immunoprecipitation-chip datasets and gene lists, see NCBI GEO submissions (http://www.ncbi.nlm.nih.gov/geo/), accession number GSE4566, and the supplemental material. For higher resolution tiling arrays, precipitated chromatin was subjected to round B amplification as described above; 5.0 μg of total DNA was fragmented into approximately 100-bp fragments by DNase I treatment and labeled with biotin (31). Labeled material was hybridized to *S. pombe* Affymetrics high-density oligonucleotide gene chips covering chromosome II and half of chromosome III (42). Data were normalized to the 50th percentile, and the binding ratio versus untagged wild type was determined as described previously (42). Normalization and data analysis were performed with Genespring 7.2 (Silicon Genetics), Access, and Excel (Microsoft) software. Complete tiling array datasets are at NCBI GEO submissions (http://www.ncbi.nlm.nih.gov/geo/), accession number GSE4566.

Cluster, hypergeometric distribution, and gene ontology analysis. Binding clusters were built with WT (H4K5Ac, H4K12Ac, H3K14Ac, H4K16Ac, and H4K9Ac) acetylation ratios corrected for H3 density together with Ssn6, Tup11, and Tup12 binding ratios (n = 4,055). Hierarchical expression clusters were built in two steps with Ssn6/Tup11/Tup12 individual common IGR- and ORF-bound targets of ≥85% (n = 334). First, all the expression levels were hierarchically clustered, and second, the relationship between experiments was built in a condition tree. All cluster analysis was performed by using a Pearson correlation algorithm with the Genespring 7.2 (Silicon Genetics) software. Significant Tup11/12- and Ssn6-specific target association with different gene ontology categories was determined using the GO miner web resource (http://discover.nci.nih.gov/gominer/) (55). Significance similarity analysis with previously published microarray data (51) was performed with the hypergeometric distribution test using the Genespring 7.2 software (Silicon Genetics).

RESULTS

Ssn6 is an essential protein in *S. pombe*. The Ssn6 protein in fission yeast is encoded by the ORF *SPBC23E6.09* on chromosome II which shows a clear match with other Ssn6 orthologues in the *Ascomycetes*. Fluorescence microscopy of a strain in which *ssn6*$^+$ is fused at the C terminus to a GFP tag (13) shows a distinct nuclear expression pattern (Fig. 1A), similar to that observed for Tup11 and Tup12 previously (13). To analyze the function of Ssn6, we created a diploid strain containing a heterozygous null allele of the *ssn6* gene by insertion of a kanamycin cassette. The resulting strain was validated by PCR and Southern blot analysis (data not shown). Interestingly, tetrad dissection of the *ssn6*$^+$//*ssn6*Δ strain revealed that only two kanamycin-sensitive spores were viable in each tetrad (Fig. 1B), and thus, Ssn6 is an essential protein under normal growth conditions in fission yeast. Viable kanamycin-resistant (*ssn6*Δ) haploid progeny can be obtained if the *ssn6*$^+$//*ssn6*Δ strain is first transformed with a plasmid expressing Ssn6 (pDual-Ssn6), and thus, the observed growth defect is associated with the *ssn6*Δ allele and its failure to produce the Ssn6 protein (Fig. 1C). These haploid progeny are uracil protrophs due to the presence of the pDual-Ssn6 plasmid which contains the *ura4*$^+$ selectable marker gene. As expected, growth of kanamycin-resistant progeny is dependent on the presence of the pDual-Ssn6 plasmid, since curing of the plasmid from the strains on 5-FOA-containing plates leads to loss of viability (Fig. 1C). The lethality does not appear to be due to defective spore germination, since microcolonies can form on YES media plates containing 1.2 M sorbitol. Images from cells obtained from microcolonies show that *ssn6*Δ cells exhibit an abnormal morphology compared to WT cells (Fig. 1D). We conclude that Ssn6 has cellular roles that are not shared by the Tup11 and Tup12 genes, since strains lacking both Tup11 and Tup12 are viable under equivalent growth conditions. Our results thus suggest the existence of a class of genes that are regulated by Ssn6 but not Tup11 or Tup12.

Ssn6 and Tup11/12 affect the regulation of distinct but overlapping sets of genes. To screen for Ssn6 regulated gene targets in *S. pombe*, we used DNA microarrays (53) to compare RNA expression profiles in a strain containing a conditional *ssn6* allele (*ssn6HA-ts*) (13) with a wild-type strain at the nonpermissive temperature. The scatter plot in Fig. 2A shows that the expression of a number of genes is affected in the *ssn6HA-ts* strain. Sixty-five genes were reduced in expression, and 29 genes were increased in expression by ≥1.8-fold. To determine whether these genes are also targets of Tup11 or Tup12, we performed a similar comparison of a *tup11*Δ *tup12*Δ double deletion strain with the wild type (Fig. 2B). Ninety-one genes were reduced in expression, and 158 genes were increased in expression by ≥1.8-fold. The number of genes affected in the *ssn6HA-ts* array was lower than in the *tup11*Δ *tup12*Δ expression profile, which could be explained by a lower penetrance of the partly functional *ssn6HA-ts* allele. We therefore used a third approach to detect potential corepressor targets in which Ssn6 was overexpressed from a plasmid. The scatter plot in Fig. 2C shows the expression profile of genes affected by Ssn6 overexpression. Two hundred seventy-nine genes were reduced in expression, and 163 genes were increased in expression by ≥2-fold. The individual genes identified in each of these experiments are listed in Table S1 in the supplemental material. Several genes showing altered expression in each of these DNA microarray studies have been studied independently by RT-PCR under the same conditions (data not shown) (13). In general, the results were in good agreement with the DNA microarray results.

To identify the group of genes that require both Ssn6 and Tup11/12 for repression, we determined the overlap between genes found in the different studies for both up- and down-regulated genes (Fig. 2D). Since the *ssn6HA-ts* allele has generally lower effects on target gene expression, we used a change threshold of ≥1.5-fold for selection of these genes (145 genes expressed at a lower level and 113 at a higher level). Each of the three sets of selected genes overlap significantly with each other, identifying common groups of genes whose expression is affected in at least two of the three conditions, but the overlaps are less pronounced for down-regulated targets, as expected for defects in a corepressor. Importantly 69 (53 + 16) genes require the function of both Ssn6 and Tup11/12. However, most of the identified genes are not found in the intersecting region affected by *ssn6HA-ts* and *tup11*Δ *tup12*Δ. It could be argued that many genes that lie outside the overlap are targets for both Ssn6 and Tup11/12 but that in one case the change in their expression lies just below the relative change threshold that we applied. This does not seem to be the case, since the relative change distribution associated with *tup11*Δ *tup12*Δ in the Ssn6-dependent group of genes (n = 189) is not significantly changed from that observed in a random set of genes

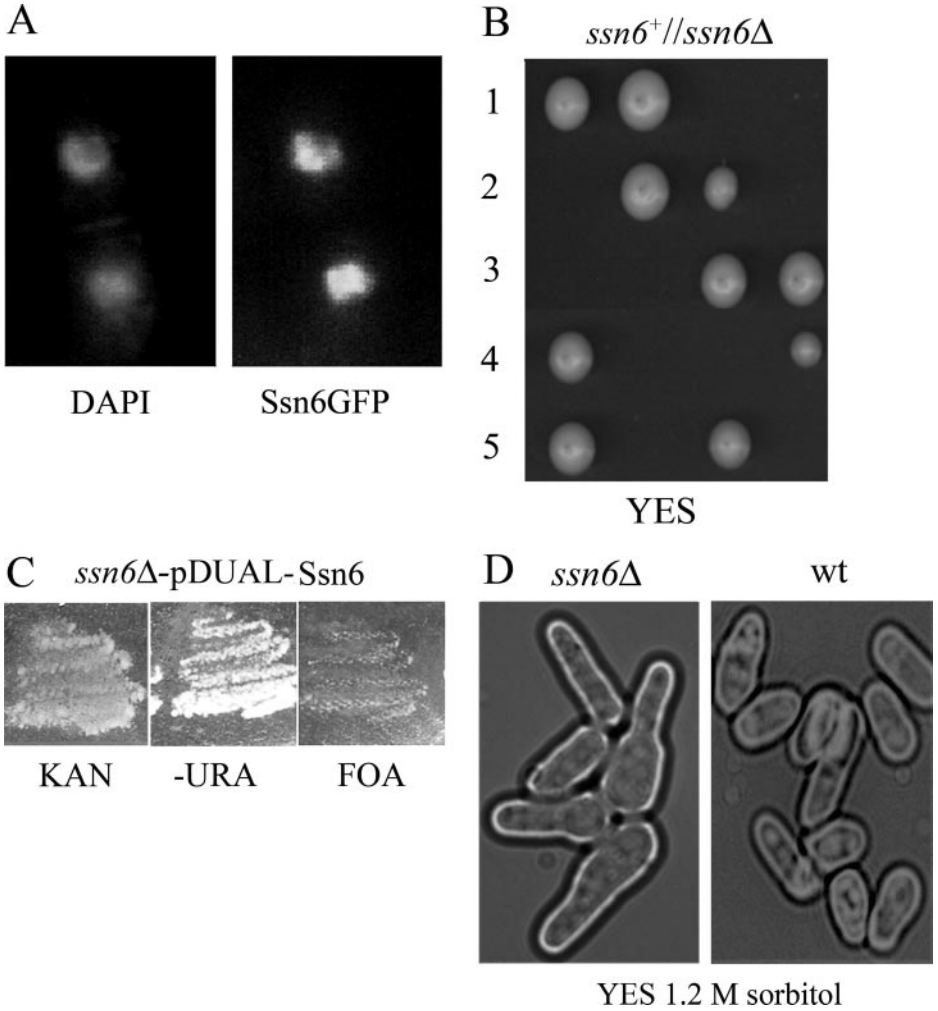

FIG. 1. The Ssn6 protein is a nuclear protein that is essential for viability in *S. pombe*. (A) Immunofluorescence microscopy analysis showing the nuclear staining pattern of the Ssn6GFP fusion protein expressed from the genomic Ssn6 locus and nuclear DNA staining of the same cell performed with DAPI. (B) Surviving spores after tetrad dissection of a heterozygous *ssn6*$^+$*//ssn6*Δ strain. Tetrad dissection results in a 50% survival ratio on rich media (YES). All surviving spores are kanamycin sensitive, indicating an essential function of the Ssn6 protein. (C) A *ura4*$^+$ plasmid expressing the full-length Ssn6 protein (pDUAL-Ssn6) can complement the *ssn6*Δ lethality phenotype. Kanamycin-resistant colonies were recovered from haploid spores containing pDUAL-Ssn6. Counterselection against pDUAL-Ssn6 with 5-FOA prevents formation of kanamycin-resistant colonies. (D) Image showing the abnormal morphology of *ssn6*Δ cells in microcolonies growing on YES with 1.2 M sorbitol together with WT control cells from normal sized colonies.

($P = 0.8$). The same is true for the observed effects of *ssn6HA-ts* in the Tup11/12-dependent targets ($n = 180$). Thus, the majority of these genes selectively require either Ssn6 or Tup11/12 for their regulation. From these studies, we conclude that Ssn6 and Tup11/12 appear to regulate overlapping but distinct groups of target genes in fission yeast.

Identification of genes directly targeted by Ssn6 and Tup11/12. The idea that Ssn6 and Tup11/12 may regulate different groups of genes assumes that the genes identified by expression profiling are primarily direct target genes that physically associate with the corepressor. To determine which corepressor subunits are localized with the gene sets identified in Fig. 2D, we used chromatin immunoprecipitation of extracts prepared from strains in which Ssn6, Tup11, and Tup12 were fused to GFP. Strains expressing the GFP-tagged proteins do not cause any detectable growth phenotypes on KCl-containing media (data not shown), a condition where *tup11*Δ *tup12*Δ and *ssn6HA-ts* cause clear phenotypes (13). Initially, we investigated the *rds1*$^+$ gene to optimize precipitation conditions. Figure 3A shows the binding ratios of the Ssn6, Tup11, and Tup12 proteins at the *rds1*$^+$ promoter relative to their association with the tRNA glutamyl synthetase promoter, which is not targeted by the corepressor. The results show strong selective precipitation of the *rds1*$^+$ fragment with all three fusion proteins, while no selective binding was observed in a nontagged control strain.

Next, we determined the genome-wide localization of the Ssn6, Tup11, and Tup12 proteins. We used DNA microarrays containing approximately 10,000 genomic fragments spotted in duplicate (51). To identify genomic regions that are significantly enriched in Ssn6, Tup11, and Tup12, we used a median percentile ranking procedure that has been described previ-

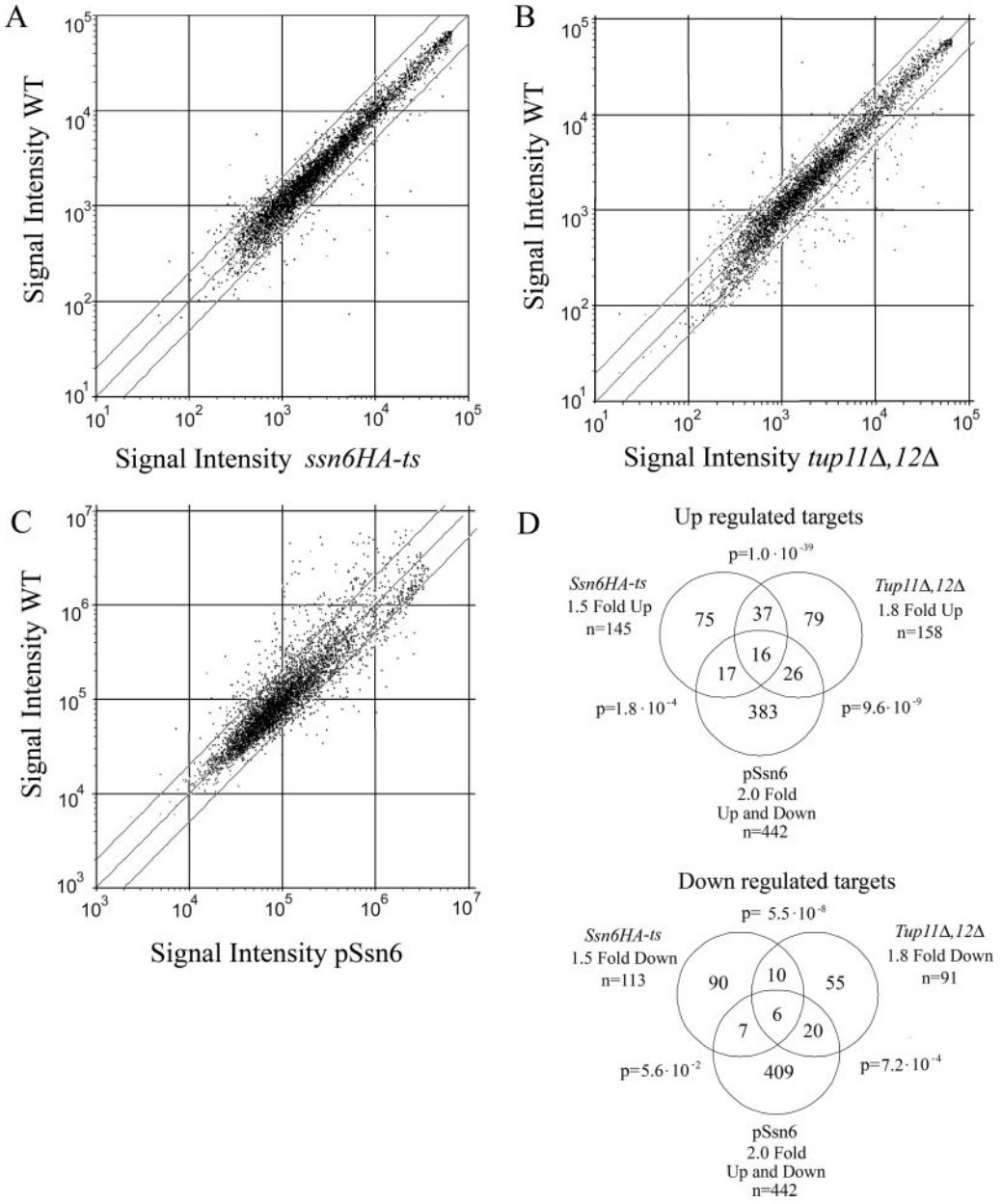

FIG. 2. Ssn6-regulated gene targets are partly distinct from Tup11/12 targets. (A) Sample control plot showing genes affected in the *ssn6HA-ts* mutant strain at 36°C. The values plotted are the averages of signals measured after hybridization of two independent sets of samples from the *ssn6HA-ts* strain and WT control after Lowess normalization. The diagonal lines show the position of signals that are the same in both samples (middle line) as well as genes whose expression is increased (lower line) or decreased (upper line) by twofold in the mutant strain. (B) Sample control plot showing genes affected in the *tup11*Δ *tup12*Δ mutant strain in relation to the wild-type control (JY741). The values plotted are the Lowess-normalized average of signals measured after hybridization of two independent sets of samples. Annotation of the plot is the same as for panel A. (C) Sample control plot showing genes affected by Ssn6 overexpression. The values plotted are the averages of signals measured after hybridization of two independent sets of samples of JY741 containing pDUAL-Ssn6 or the pDUAL-Empty control after Lowess normalization. Annotation of the plot is the same as for panel A. (D) Venn diagrams showing the overlap between up-regulated and down-regulated genes affected in the *ssn6HA-ts* (≥1.5-fold) and in the *tup11*Δ *tup12*Δ (≥1.8-fold) mutant strains together with all genes affected by Ssn6 overexpression (≥2.0-fold). The overlaps between the up-regulated gene sets are all significantly larger than would be expected by chance ($P = 1.0 \times 10^{-39}$, 9.6×10^{-9}, and 1.8×10^{-4}, respectively) and notably larger than the overlaps between the down-regulated gene sets ($P = 5.5 \times 10^{-8}$, 7.2×10^{-4}, and 5.6×10^{-2}, respectively).

ously (5). Figure 3B shows the distribution of the median percentile-ranked binding ratios for Ssn6, Tup11, and Tup12. Fragments significantly enriched in Ssn6, Tup11, or Tup12 lie outside the normal distribution described by the bulk of the data. We selected genes within the 85th percentile and above for further analysis. Lists of these genes are shown in Table S2 in the supplemental material. To identify direct corepressor targets, we studied the overlap between the group of genes that

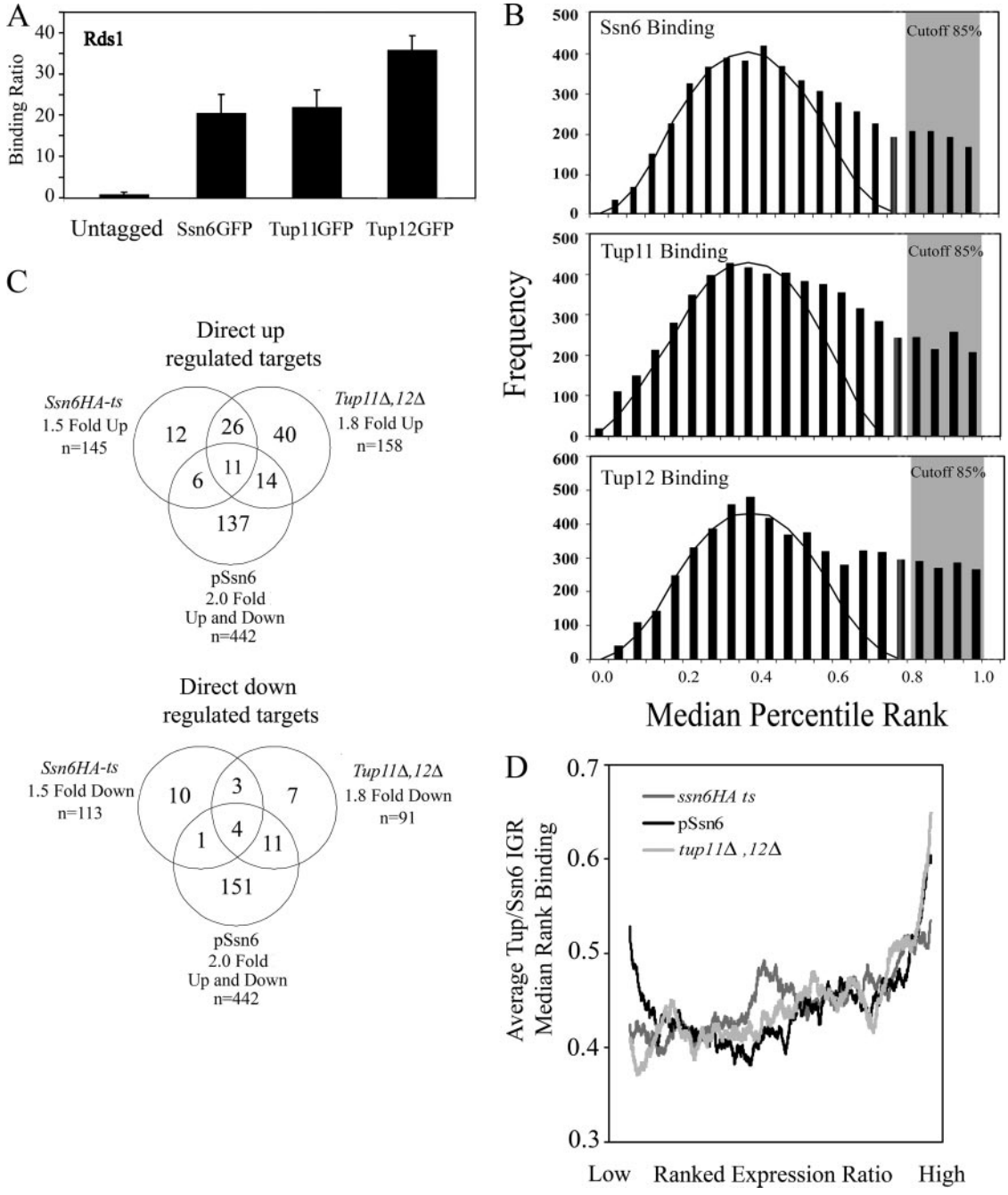

FIG. 3. Genome-wide localization of Ssn6, Tup11, and Tup12 correlates with the localization of genes whose expression is affected by *ssn6HA-ts*, *tup11*Δ *tup12*Δ, and Ssn6 overexpression. (A) Ssn6, Tup11, and Tup12 are specifically associated with the *rds1*$^+$ promoter in chromatin immunoprecipitation experiments. Binding to the *rds1*$^+$ promoter (mean of triplicate samples ± standard error) was calculated in relation to binding observed for the tRNA glutamyl synthetase promoter that was used as a control. The bars show the relative level of precipitated *rds1*$^+$ chromatin fragments after quantification by SYBR green real-time PCR. (B) Identification of genomic regions that are significantly associated with Ssn6GFP, Tup11GFP, and Tup12GFP. The histograms represent the frequencies of median ranked binding ratios of precipitated chromatin fragments in relation to input levels. The gray zones above the 85th percentile indicate targets outside the normal distribution (black line) that were classified as bound targets. A complete list of enriched fragments is found in Table S2 in the supplemental material. (C) Many genes whose expression is dependent on Ssn6 or Tup11/12 or affected by Ssn6 overexpression are direct corepressor targets. The Venn diagrams show the correspondence between overlapping groups of up- and down-regulated genes affected by corepressor defects or Ssn6 overexpression (Fig. 2D) with genes bound by Ssn6, Tup11, or Tup12 (≥85th percentile, $n = 953$). (D) The genomic distribution of corepressor subunits correlates with the localization of genes regulated by Ssn6 and Tup11/12. Moving average plot showing average binding level of Ssn6, Tup11, and Tup12 to intergenic regions of all genes (median rank binding) after ranking of the genes according to the effects on gene expression caused by *ssn6HA-ts*, tup11Δ *tup12*Δ, and Ssn6 overexpression (ranked expression ratio). The window size for the moving average plot was 100.

physically interact with one or more corepressor subunits (≥85th percentile binding) (Fig. 3B) and the groups of genes whose expression levels depend on Ssn6 or Tup11/12 or whose expression is affected by Ssn6 overexpression (Fig. 2D). Figure 3C shows that many up- and down-regulated targets identified by expression profiling are also physically associated with the corepressor. We observe a bias for binding to up-regulated targets, but altogether, about one-third of expression targets are bound by corepressor components. This is likely to be an underestimate, since the ≥85th percentile selection provides a very conservative estimate of binding targets. Furthermore, it is likely that corepressor components bind to regions that are not covered by the probes on the DNA microarray.

To further investigate the global relationship between corepressor function and its genome-wide localization, we plotted moving averages of the combined binding data after ranking the IGR of the genes according to their expression ratio in each of the three expression profiling studies. Figure 3D shows that genes that are derepressed in the *ssn6HA-ts* and *tup11*Δ *tup12*Δ mutant strains (high expression ratio) are correlated with IGRs with elevated levels of corepressor binding. Genes that are repressed by Ssn6 overexpression (low expression ratio) are also highly correlated with IGRs that show high levels of corepressor binding. Thus, groups of genes from each of the three expression profiling experiments that are putative targets for corepressor-dependent repression are enriched in genes that bind to the corepressor. Interestingly, the group of genes whose expression is increased by Ssn6 overexpression (high expression ratio) is also associated with direct corepressor binding. The possible significance of this correlation is discussed in Discussion. The high level of correlation between the functional significance of corepressor subunits and their localization allows the selection of sets of genes in the ensuing sections whose target gene status is supported by both functional and binding data.

Corepressor components colocalize in both the intergenic and coding regions of genes. We have shown that genes whose expression is differentially dependent on Ssn6 and Tup11/12 are bound by corepressor subunits and are thus likely to be direct targets. The differential dependence of different genes on Ssn6 and Tup11/12 could in principle depend on factors such as differential localization of the corepressor within target genes. Alternatively, different versions of the corepressor, containing different combinations of subunits, could be associated with different genes. To address these possibilities, we first investigated the nature of the locations to which Ssn6, Tup11, and Tup12 are bound. About half the probes on the DNA microarray correspond to ORFs. Even though the corepressor shows a preference for localization within IGRs, it is also frequently found in the ORF regions of genes (Fig. 4A). In the majority of cases, the corepressor was found associated with either the IGR or the ORF of individual genes. This, together with the lack of any detectable tendency for the identified ORFs to be adjacent to downstream corepressor-bound IGRs, shows that the apparent binding to ORF fragments is not an artifact resulting from its association with nearby corepressor-bound IGRs. We conclude that Ssn6, Tup11, and Tup12 are associated with both IGRs and ORFs. We next studied the relative localization of Ssn6, Tup11, and Tup12 in the genome. Figure 4B shows a very high overlap in the localization of the proteins. However, there is a significant number of fragments that are identified in only one of the data sets by the selection criteria used (≥85th percentile binding). Thus, either differential localization within target gene or differential subunit composition provides a possible explanation that could account for target gene-selective roles of Ssn6 and Tup11/12. These possibilities are investigated in detail below.

To study the relative localization of Ssn6, Tup11, and Tup12 quantitatively at IGRs and ORFs, we independently calculated percentile ranked binding to fragments of each type (see Table S2 in the supplemental material). The distribution of IGR binding levels for Ssn6, Tup11, and Tup12 in each of the individually selected gene sets shows that each of the binding distributions is clustered high in the median rank and contrasts strongly with a randomly selected set of genes (Fig. 4C). The vast majority of Ssn6-bound genes are also associated with Tup11 and Tup12, since ≥75% of Ssn6-bound genes are found within the top 10% of Tup11- and Tup12-bound genes. A similar relationship is seen between Tup11 and Tup12, suggesting a very strong correlation in their localization. This correlation extends to Ssn6, but here the 75th percentile lies just below 0.8 in the median rank. This pattern suggests that Tup11 and Tup12 may be bound to some targets in the absence of Ssn6. To look more closely at corepressor-bound locations where one or two subunits might be absent, we performed cluster analysis of genes from the three sets where the binding level of one or both the other subunits was below the 55th percentile (Fig. 4D). Importantly, there are almost no Ssn6-bound genes that pass these criteria. For Tup11 and Tup12, there is a slightly larger number of genes where the proteins might exist alone or in association with only one other corepressor subunit. Taken together, these results suggest that the vast majority of corepressor-bound locations are associated with all three corepressor subunits and that Ssn6 selective repression is most likely mediated via corepressors containing Ssn6, Tup11, and Tup12 subunits.

To allow direct comparison of Ssn6, Tup11, and Tup12 binding to IGRs and ORFs, ORF fragments with binding levels in the top 15% were selected (see Table S2 in the supplemental material). The main conclusion of these data (Fig. 4E) is that all three corepressor components show a strong tendency to colocalize on ORF binding sites, just as they do on IGRs. The ORF data are more consistent with the possibility that a minority of corepressor binding sites may not be associated with all three corepressor components than the IGR binding results (Fig. 4F). For example, there are 21 Ssn6-bound ORF sites that may lack one or both the Tup11 and Tup12 proteins compared to 3 IGR sites detected using equivalent criteria. However, this difference may be a consequence of the fact that the level of binding to ORFs tends to be somewhat lower than to IGRs (Fig. 4A). We conclude that the vast majority of corepressor binding sites are bound by all three subunits, consistent with a single predominant form of the Ssn6-Tup11/12 corepressor. Furthermore, the differential requirement for Ssn6 and Tup11/12 at different target genes cannot be due to binding of partial corepressor complexes, since there is good support for binding of all three subunits to most of these genes.

High-resolution binding maps of Tup11, Tup12, and Ssn6. As suggested above, a second mechanism by which Ssn6 and Tup11/12 could differentially affect target genes is the distri-

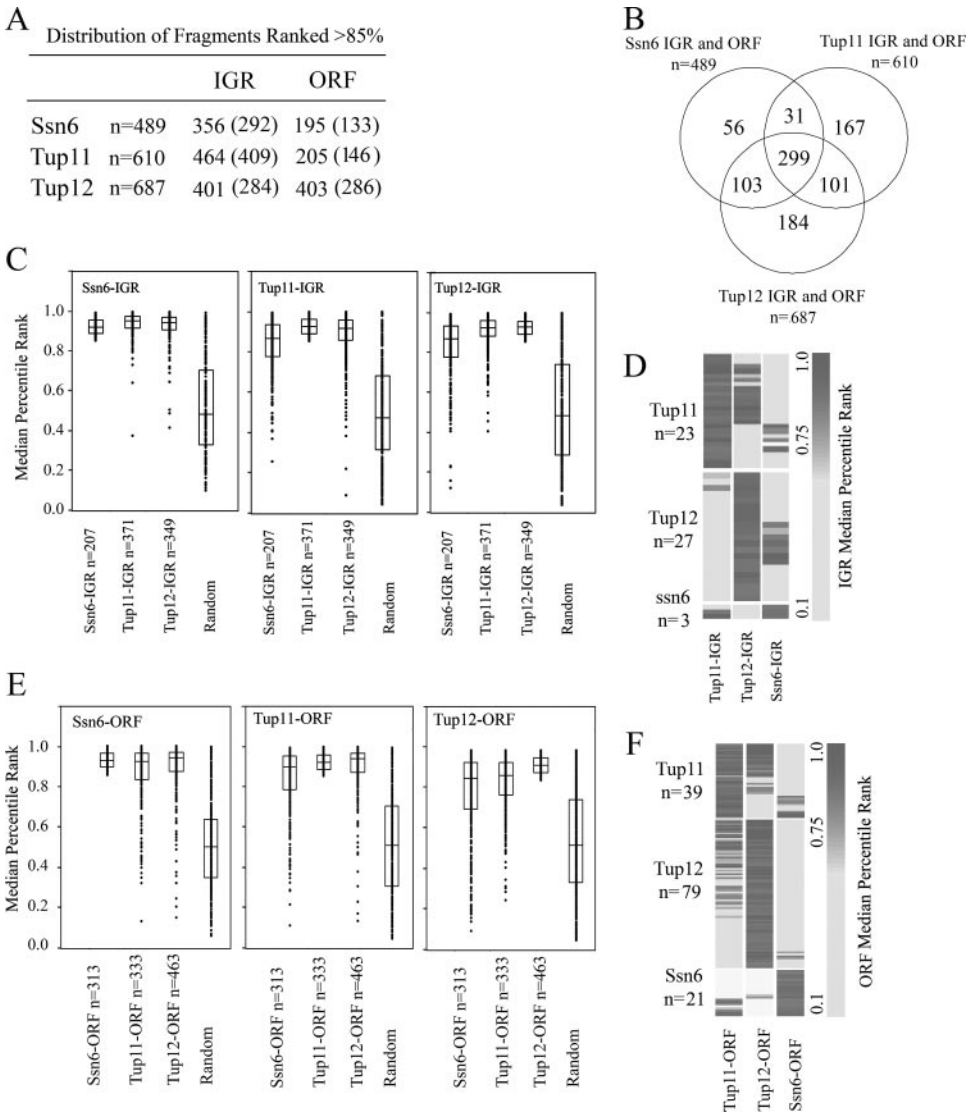

FIG. 4. Ssn6, Tup11, and Tup12 colocalize within intergenic regions and open reading frames. (A) Corepressor subunits are bound to both IGRs and ORFs. The number of fragments (≥85th percentile binding) that are bound to IGRs and ORFs, respectively, are shown. The numbers in parentheses indicate the number of genes for which binding is only observed in either the IGR or the ORF regions of genes. (B) The genomic localization of Ssn6, Tup11, and Tup12 is highly correlated. The diagram shows the overlap in the localization of the individually selected Ssn6-, Tup11-, and Tup12-bound locations. (C) Quantitative evaluation of binding by each of the three corepressor subunits to the sets of IGRs that individually show binding of Tup11, Tup12, or Ssn6 (≥85% percentile median ranked binding) confirms a very high degree of subunit colocalization in IGRs. The individual values are plotted, and the boxes show the 75th percentile, the median, and the 25th percentile for each data set. A control group containing an equivalent number of randomly selected IGRs is analyzed in each panel. (D) Very few corepressor-bound IGRs provide evidence for binding of two or fewer subunits. IGRs where fewer than three subunits may be associated were analyzed by cluster analysis. The number of genes bound by each of the subunits but where binding of one or both of the other subunits has a binding level within the lower 55% of the median binding rank is shown. (E) Quantitative evaluation of binding by each of the three corepressor subunits to the sets of ORFs that individually show binding of Tup11, Tup12, or Ssn6 (≥85% percentile median ranked binding) confirms a very high degree of subunit colocalization in ORFs. Annotation of the diagram is as for panel C, except that ORF locations are analyzed. (F) Very few corepressor-bound ORFs provide evidence for binding of two or fewer subunits. Annotation of the diagram is as for panel D, except that ORF locations are analyzed.

bution of the corepressor complex within target genes. However, the array platform used so far might not reveal such differences, since it contains only one IGR and ORF probe per gene. To investigate the localization of Ssn6, Tup11, and Tup12 with higher resolution, we used high-density tiling arrays covering *S. pombe* chromosome 2 and half of chromosome 3 with a 250-bp resolution, as described previously (42). Corepressor-bound genes were defined as those with a ≥2-fold enrichment of Ssn6, Tup11, or Tup12 anywhere within the upstream or coding region of the genes in relation to an untagged control strain.

Figure 5 shows tiling array binding profiles for a group of genes that are dependent on both Ssn6 and Tup11/12 as well as groups that are dependent on either Ssn6 or Tup11/12 and a group that is affected by Ssn6 overexpression. Expression levels for the representative genes shown under the different condi-

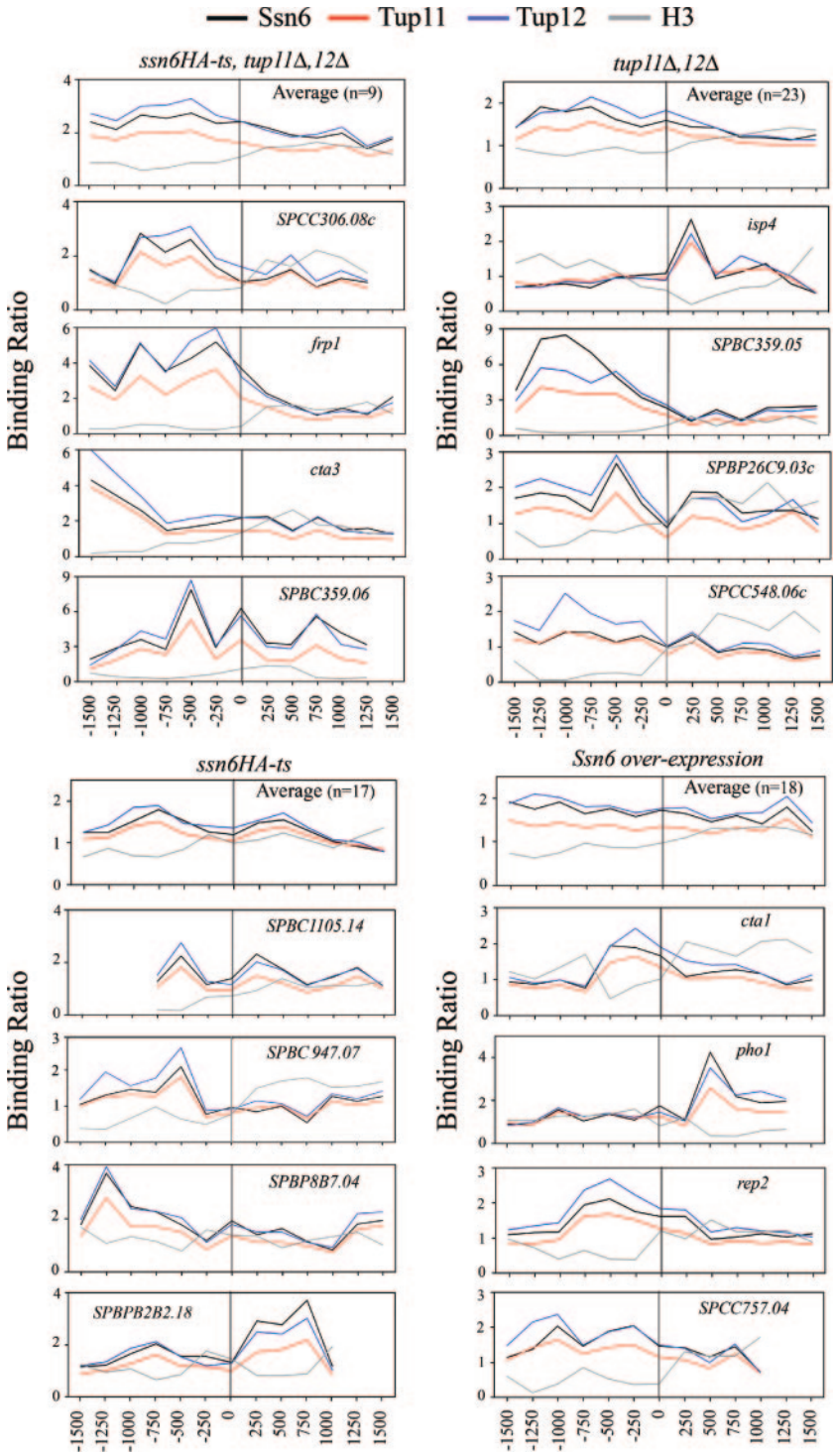

FIG. 5. Distribution of bound Ssn6, Tup11, and Tup12 in the upstream and coding regions of different classes of corepressor-regulated genes. Corepressor subunits colocalize in the IGR and/or ORF regions of genes that are dependent on either Ssn6 and/or Tup11/12 as well as genes that are affected by Ssn6 overexpression. The four major panels show the localization of Tup11, Tup12, and Ssn6 using tiling arrays with a resolution of 250 bp. The average binding distribution of Ssn6, Tup11, and Tup12 for each gene class is shown in the upper panel of each of the major panels (the number of genes used to calculate the mean profiles is shown in parentheses). As a control, the level of histone H3 binding is shown. The genes in each group were selected as genes affected ≥2-fold in expression arrays and with a tiling binding ratio ≥2 at one or more points in the analyzed promoter and coding region. The lower panels in each major panel show a selection of individual genes for each group. The binding ratio was calculated as the binding signal for Ssn6GFP, Tup11GFP, and Tup12GFP relative to an untagged WT control. Expression ratios showing the dependency of these genes on Ssn6 and Tup11/12 as well as the effect of Ssn6 overexpression are listed in Table S2 in the supplemental material.

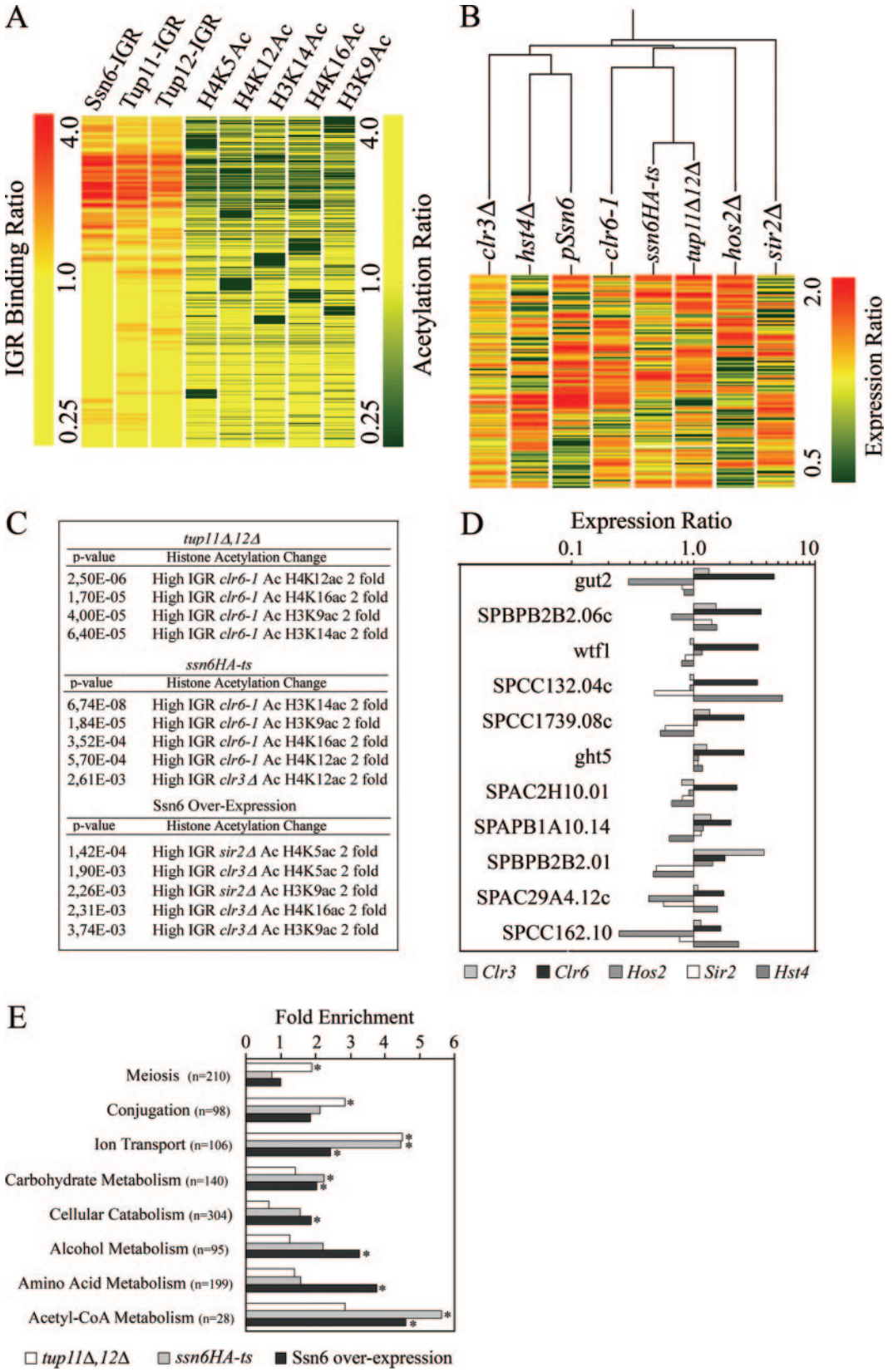

FIG. 6. Different classes of direct gene targets of the Ssn6-Tup11/12 corepressor are differentially targeted by HDACs and are enriched in different functional classes of genes. (A) Ssn6, Tup11, and Tup12 are associated with hypoacetylated regions of chromatin. Gene cluster showing Ssn6, Tup11, and Tup12 binding ratios clustered together with acetylation levels for histone H4K5Ac, H4K12Ac, H3K14Ac, H4K16Ac, and H3K9Ac (corrected for H3 occupancy) at IGRs (n = 4,055). (B) Direct corepressor target genes tend to be regulated by a specific subset of

tions are presented in Table S3 in the supplemental material. The upper panel in each group shows the mean distribution of the three proteins on genes in the group, while the lower panels show the binding patterns associated with selected individual genes within each group. As a control, each set also shows the relative levels of histone H3, which has been published previously (51). The most striking conclusion from these studies is the similarity of the binding distributions observed for Ssn6, Tup11, and Tup12, providing further strong evidence for the binding of a corepressor complex containing all three subunits. The average distribution patterns generally show higher binding in the IGR than in ORFs, but the data from this platform confirm significant binding of the corepressor to both IGR and ORF regions of regulated genes. The observed distributions are specific for the corepressor subunits because the histone H3 control pattern is generally higher in ORF regions than in IGRs. Maximal corepressor binding differs only slightly between the different groups, with a binding peak approximately 500 to 1,000 bp upstream of the ORF. The significance of such differences is unclear, since the binding patterns vary greatly for individual genes within each group. We therefore conclude that there are no simple differences in corepressor distribution that can account for the differential requirement for Ssn6 and Tup11/12 or the selective effects of Ssn6 overexpression at different gene targets.

Ssn6- and Tup11/12-dependent genes are primarily hypoacetylated and repressed by Clr6. The Ssn6-Tup1 corepressor has been shown to recruit HDACs to sites in chromatin and to bind to hypoacetylated N termini of histone proteins (10, 12). Differences associated with differential modification of chromatin could therefore account for the differential roles of Ssn6 and Tup11/12 in targeting genes for repression. To investigate the genomic localization of the corepressor in relation to genome-wide patterns of histone acetylation, we clustered the IGR binding ratios for Ssn6, Tup11, and Tup12 with previously published acetylation profiles for a range of histone acetylation sites (H4K5Ac, H4K12Ac, H3K14Ac, H4K16Ac, and H4K9Ac) corrected for H3 occupancy (51). Interestingly, a large cluster of Ssn6-, Tup11-, and Tup12-bound IGRs shows a striking correlation with a large proportion of the IGRs that are hypoacetylated at one or more of the modification sites tested (Fig. 6A). Importantly, Fig. 6A also shows data for clusters of hypoacetylated regions that are not bound by the corepressor, and therefore, corepressor binding to hypoacetylated chromatin is selective, as expected for a coregulator recruited by regulatory transcription factors.

We next asked whether Ssn6- and Tup11/12-regulated genes require different classes of HDAC enzymes for repression. Figure 6B shows a hierarchical gene tree cluster analysis of the gene expression changes at corepressor-bound genes that are affected by *ssn6HA-ts*, *tup11*Δ, *tup12*Δ, and Ssn6 overexpression together with changes associated with defects in a range of HDAC enzymes that have been published previously (51) and Hst4, which was determined in this study. The data sets from Ssn6- and Tup11/12-dependent genes cluster together in a main branch together with the expression profiles associated with the class I HDAC Clr6. Interestingly, a second branch contains the Ssn6 overexpression profile together with the profiles associated with the class III HDAC Hst4 and the class II HDAC Clr3.

A prediction of these results is that Clr6 should be the major HDAC responsible for deacetylation of Ssn6- and Tup11/12-regulated genes. To test this, we determined the relationship of the overlap between binding targets that are affected by *ssn6HA-ts*, *tup11*Δ, *tup12*Δ, or Ssn6 overexpression (see Table S4 in the supplemental material) with lists of IGR that require the function of different HDACs for their deacetylation (51). Note that data for Hst4 are not available. Figure 6C shows that Ssn6- and Tup11/12-dependent targets genes show a highly significant overlap with IGRs that require Clr6 for their deacetylation at several acetylation sites. Genes affected by Ssn6 overexpression significantly overlap with genes that are deacetylated by Clr3 and Sir2. These data independently support the conclusion from Fig. 6B that Ssn6 and Tup11/12 selective target genes tend to be targets for regulation by Clr6, while genes affected by Ssn6 overexpression tend to be regulated by class II and class III HDACs.

The association of Clr6 with corepressor-regulated genes shows that Clr6 is frequently involved in repression of these genes, but it does not exclude the involvement of other HDACs. We therefore investigated the effect of different HDACs on the expression of individual genes that were specifically deacetylated ≥2-fold by Clr6 and require Ssn6 and Tup11/12 for their repression (see Table S5 in the supplemen-

HDACs. Hierarchical two-dimensional expression cluster analysis of gene expression changes caused by *ssn6HA-ts*, *tup11*Δ *tup12*Δ, and Ssn6 overexpression as well as mutations defective in different HDACs. The clustered genes also exhibit high binding in the IGR or ORF (≥85th percentile) for each of Ssn6, Tup11, and Tup12 ($n = 334$). The reciprocals of the Ssn6 overexpression data are shown to allow easier comparison with the other conditions. (C) Direct corepressor target genes depend on a subset of HDACs for deacetylation of histones in their upstream IGRs. The tables show the significance (P values) of overlaps between direct targets of Ssn6 (≥1.5-fold expression change in *Ssn6HA-ts*, ≥75% Ssn6 IGR binding), Tup11/12 (≥1.8-fold expression change in *tup11*Δ *tup12*Δ, ≥75% Tup12 IGR binding), and by Ssn6 overexpression (≥2.0-fold expression change, ≥75% Ssn6 IGR binding) with groups of genes that depend on different HDACs for deacetylation (≥2-fold) of different histone residues within their IGRs (47). (D) The Clr6 HDAC plays the major role in the repression of individual genes that are directly targeted by Ssn6HA and Tup11/12 and are deacetylated by Clr6, but Clr3 and Hst4 are also involved in repression of some of the genes. The bar graph shows the expression changes resulting from defects caused by different mutant HDACs published previously (51) and for *hst4*Δ (this study). A list of all Ssn6HA and Tup11/12 targets that are dependent on Clr6 for deacetylation (≥2-fold, $n = 34$) are listed in Table S5 in the supplemental material. (E) Genes dependent on Ssn6 (≥1.5-fold expression change in *Ssn6HA-ts*, ≥75% IGR or ORF binding) or Tup11/12 (≥1.8-fold expression change in *tup11*Δ *tup12*Δ, ≥75% IGR or ORF binding) and genes affected by Ssn6 overexpression (≥2.0-fold expression, ≥75% IGR or ORF binding) are enriched in genes from different functional categories. Selected gene ontology process categories that are significantly enriched in gene sets targeted by Ssn6 and/or Tup11/12 are shown. The bars show the extent of category enrichment in the Ssn6 and Tup11/12 target groups relative to their genomic frequency. Significantly enriched categories ($P < 0.05$) are indicated (*). The gene sets analyzed and the complete GO category analysis are presented in Table S6 in the supplemental material.

tal material). Clr6 is the only HDAC that contributes significantly to the repression of most of these genes. Interestingly, Hst4 and Clr3 played a significant role in repression of a minority of the genes. These are the same class II and class III HDACs that were associated with corepressor targets affected by Ssn6 overexpression.

One explanation for the existence of selective gene targets for Ssn6 and Tup11/12 is that the selective aspects of corepressor function have coevolved together with the evolution of genes involved in distinct cellular functions. To test this possibility, we sought to determine whether sets of Ssn6HA-ts- and Tup11/12-dependent gene targets, as well as gene sets affected by Ssn6 overexpression were significantly enriched in any of the gene ontology (GO) process terms. We found GO categories that are selectively and specifically overrepresented in the different groups as well as some categories that were significantly enriched in all groups (Fig. 6E). Both the Ssn6- and Tup11/12-dependent genes were selectively enriched in functional categories involved in ion transport, conjugation, and carbohydrate metabolism among other categories. Interestingly, Tup11/12-dependent targets were selectively enriched in the meiosis category but played a subsidiary role in the cellular catabolism, alcohol metabolism, and amino carbohydrate categories. A complete list of the three groups of genes and the associated GO categories can be found in Table S6 in the supplemental material. We conclude that selective gene targets dependent on Ssn6 and Tup11/12 and those affected by Ssn6 overexpression are enriched significantly for different classes of genes that contain genes involved in distinct cellular processes.

DISCUSSION

In *S. cerevisiae*, Ssn6 has been shown to be a bridging component of the Ssn6-Tup1 complex that connects the repression activity found in the Tup1 protein to DNA-bound repressor proteins in the regulatory regions of target genes (46). Our studies of Ssn6 in *S. pombe* provide important new insights into the function of Ssn6, which are likely to be significant for understanding corepressors in other organisms, including *S. cerevisiae* and higher eukaryotes. First, the essential nature of the *S. pombe* Ssn6 protein suggests an active repression role of Ssn6 in addition to the repressive activity associated with Tup11/12 because a strain lacking both Tup11 and Tup12 is viable. Since the Tup11/12-independent function of Ssn6 is likely to involve gene regulation, we used DNA microarray analysis of a temperature-sensitive *ssn6HA-ts* strain to identify Ssn6 targets. Comparison of Ssn6-dependent target genes with genes that require Tup11 and/or Tup12 for correct expression showed that many targets require both Ssn6 and Tup11/12 subunits for repression, while many others are selectively dependent on either Ssn6 or Tup11/12. Thus, the Ssn6 and Tup11/12 components of the corepressor appear to have distinct but overlapping functions that are manifested by differences in the phenotype of mutant strains as well as in their target genes. Interestingly, similar findings have been reported for *C. albicans* where Ssn6 and Tup1 play different roles in dimorphic growth (16, 22). DNA microarray studies of *tup1*Δ and *ssn6*Δ mutants in *S. cerevisiae* have shown a highly significant overlap in the target genes that require each protein for their correct regulation (21). However, 40% of Ssn6 targets and 15% of Tup1 targets in this study do not overlap if a twofold threshold is used to select putative corepressor target genes using these *S. cerevisiae* datasets. Thus, there may also be a difference in the sets of genes targeted by Ssn6 and Tup1 in *S. cerevisiae* even though the difference is less pronounced than in *S. pombe* and *C. albicans*.

The identification of target genes that are selectively regulated by Ssn6 and Tup11/12 suggested the possibility that the corepressor components could be recruited to some genes independently of each other. The high degree of overlap between the localization data for Ssn6, Tup11, and Tup12 suggest that this is not the case. The overlap is seen most clearly in data for the higher resolution tiling arrays where changes in binding of Ssn6, Tup11, and Tup12 between adjacent probe locations are highly correlated. For the vast majority of genes that are selectively regulated by Ssn6 or Tup11/12, there is strong evidence for binding of all three components of the corepressor. Therefore, selective repression of gene targets by Ssn6 or Tup11/12 must be accounted for in the context of recruited repressor complexes containing all three subunits. However, the nature of genome-wide localization data makes it difficult to categorically exclude the existence of corepressor forms containing fewer than three of the subunits. Our data provide little if any clear evidence for recruitment of Ssn6 in the absence of Tup11 or Tup12. There is a larger set of genes that may be associated with Tup11 and/or Tup12 in the absence of Ssn6. Interestingly, Tup1 has previously been shown to interact with the Matα2 repressor protein independently of Ssn6 in *S. cerevisiae* (28). Even though all three corepressor subunits are generally colocalized in the wild type, our gene-profiling results predict that Ssn6 should be recruited to Ssn6-selective genes in strains lacking Tup11 and Tup12. Tup11/12-independent recruitment of Ssn6 is consistent with the known ability of Ssn6 to interact directly with DNA-bound repressor proteins (see the introduction), but the Tup11/12 dependency of its recruitment will be tested directly in future studies.

Ssn6, Tup11, and Tup12 are localized in regions of the genome that are relatively underacetylated on histone residues, most significantly H3-K14, H4-K5, H4-K12, and H4-K16. The overlap between Ssn6- and Tup11/12-dependent genes and genes that are deacetylated and regulated by Clr6 suggests that Clr6 is the major HDAC regulating Ssn6- and Tup11/12-repressed genes. Indeed, Clr6 could be recruited to these genes by the Ssn6-Tup11/12 corepressor, as has been shown for the analogous system in *S. cerevisiae* (50). Interestingly, histone H4-K5, which is underacetylated in Ssn6 and Tup11/12 target genes, does not seem to require Clr6 for deacetylation in these genes. In *S. cerevisiae*, hypoacetylation of Ssn6-Tup1 target genes has been associated with the class II HDAC Hda1 (40). In our data, the Hda1 orthologue in *S. pombe*, Clr3, and class III HDACs are required for deacetylation of acetylated histone residues (including H4-K5Ac) within corepressor target genes that are affected by Ssn6 overexpression as well as their repression. Although Clr6 is the only HDAC that is required for repression of many Ssn6-, Tup11/12-, and Clr6-dependent genes, a group of these genes are also derepressed by defects in Clr3 and the class III HDAC Hst4. To our knowledge, this is the first report associating class III HDACs in the repression of Ssn6-Tup1 targeted genes.

We used Ssn6 overexpression as a complementary approach to identify corepressor target genes because the number of genes affected by *ssn6HA-ts* and the extent of the changes in their expression was much less than for *tup11*Δ *tup12*Δ. Although the mechanism by which Ssn6 overexpression influences corepressor activity is unclear, the genes identified show significant overlaps with Ssn6 and Tup11/12 genes as well as localization data for corepressor subunits. As for Ssn6- and Tup11/12-dependent genes, the analysis of corepressor target genes in this work is exclusively based on Ssn6 overexpression target genes for which there is strong independent evidence of corepressor binding. Interestingly, many corepressor binding target genes are up-regulated in response to Ssn6 overexpression. Although a range of mechanisms could account for this result, it is possible that the corepressor complex adopts a coactivator function under some conditions in *S. pombe*. Previous work with *S. cerevisiae* has suggested such a coactivator role for the Tup1-Ssn6 complex (7, 27).

Many previous studies have shown that the Ssn6-Tup1 corepressor complex is recruited to regulatory sites in the intergenic regions of the genome by DNA-bound repressor proteins. Consistently, we find the fission yeast corepressor preferentially located in the upstream region of genes. In the tiling microarray data, we often see sharp peaks in the level of corepressor, as would be expected for recruitment to specific upstream sites by repressor proteins. Surprisingly, however, we also see binding of Ssn6, Tup11, and Tup12 to sites in the transcribed regions of genes. Some HDACs, such as Hos2 and Rpd3, are also associated with the transcribed regions of genes (6, 49, 51). The RNA polymerase II mediator complex, which is also a target for Ssn6-Tup1-mediated repression in *S. cerevisiae*, has also recently been identified in the transcribed region of genes in *S. cerevisiae* and *S. pombe* (2, 58). It is thus possible that Ssn6-Tup11/12 recruits HDACs and/or the mediator complex to transcribed regions or that it is recruited by one of these components to this location. The functional significance of Ssn6-Tup11/12 corepressors in transcribed regions will be the subject of future studies.

ACKNOWLEDGMENTS

We thank Akihisa Matsuyama and Minoru Yoshida at the Chemical Genetics Laboratory, Riken, Saitama, Japan, for providing plasmids for expression of the Ssn6 protein. We also thank members of the Wright and Ekwall groups for valuable discussions and advice on the manuscript.

DNA microarray slides were scanned at the KI-CHIP core facility at the Karolinska Institute, which is supported by the Wallenberg Foundation. Affymetrics tiling arrays were hybridized and scanned at BEA Bioinformatics and Expression Analysis Core Facility, Karolinska Institute.

This research was funded by project grants from the Swedish Research Council and the Foundation for Strategic Research. A.P.H.W. is a senior investigator financed by the Swedish Research Council. K.E. is a Royal Swedish Academy of Sciences research fellow supported by the Knut and Alice Wallenberg foundation, Swedish Cancer Society, and the Swedish Research Council.

REFERENCES

1. **Alfa, C., P. Fantes, J. Hyams, M. McLeod, and E. Warbrick.** 1993. Experiments with fission yeast: a laboratory course manual. Cold Spring Harbor Laboratory Press, Plainview, NY.
2. **Andrau, J. C., L. van de Pasch, P. Lijnzaad, T. Bijma, M. G. Koerkamp, J. van de Peppel, M. Werner, and F. C. Holstege.** 2006. Genome-wide location of the coactivator mediator: binding without activation and transient Cdk8 interaction on DNA. Mol. Cell **22:**179–192.
3. **Bahler, J., J. Q. Wu, M. S. Longtine, N. G. Shah, A. McKenzie III, A. B. Steever, A. Wach, P. Philippsen, and J. R. Pringle.** 1998. Heterologous modules for efficient and versatile PCR-based gene targeting in Schizosaccharomyces pombe. Yeast **14:**943–951.
4. **Bjerling, P., R. A. Silverstein, G. Thon, A. Caudy, S. Grewal, and K. Ekwall.** 2002. Functional divergence between histone deacetylases in fission yeast by distinct cellular localization and in vivo specificity. Mol. Cell. Biol. **22:**2170–2181.
5. **Buck, M. J., and J. D. Lieb.** 2004. ChIP-chip: considerations for the design, analysis, and application of genome-wide chromatin immunoprecipitation experiments. Genomics **83:**349–360.
6. **Carrozza, M. J., B. Li, L. Florens, T. Suganuma, S. K. Swanson, K. K. Lee, W. J. Shia, S. Anderson, J. Yates, M. P. Washburn, and J. L. Workman.** 2005. Histone H3 methylation by Set2 directs deacetylation of coding regions by Rpd3S to suppress spurious intragenic transcription. Cell **123:**581–592.
7. **Conlan, R. S., N. Gounalaki, P. Hatzis, and D. Tzamarias.** 1999. The Tup1-Cyc8 protein complex can shift from a transcriptional co-repressor to a transcriptional co-activator. J. Biol. Chem. **274:**205–210.
8. **Cooper, J. P., S. Y. Roth, and R. T. Simpson.** 1994. The global transcriptional regulators, SSN6 and TUP1, play distinct roles in the establishment of a repressive chromatin structure. Genes Dev. **8:**1400–1410.
9. **Davie, J. K., D. G. Edmondson, C. B. Coco, and S. Y. Dent.** 2003. Tup1-ssn6 interacts with multiple class I histone deacetylases in vivo. J. Biol. Chem. **278:**50158–50162.
10. **Davie, J. K., R. J. Trumbly, and S. Y. Dent.** 2002. Histone-dependent association of Tup1-Ssn6 with repressed genes in vivo. Mol. Cell. Biol. **22:**693–703.
11. **Edmondson, D. G., and S. Y. Roth.** 1998. Interactions of transcriptional regulators with histones. Methods **15:**355–364.
12. **Edmondson, D. G., M. M. Smith, and S. Y. Roth.** 1996. Repression domain of the yeast global repressor Tup1 interacts directly with histones H3 and H4. Genes Dev. **10:**1247–1259.
13. **Fagerstrom-Billai, F., and A. P. Wright.** 2005. Functional comparison of the Tup11 and Tup12 transcriptional corepressors in fission yeast. Mol. Cell. Biol. **25:**716–727.
14. **Flores-Saaib, R. D., and A. J. Courey.** 2000. Analysis of Groucho-histone interactions suggests mechanistic similarities between Groucho- and Tup1-mediated repression. Nucleic Acids Res. **28:**4189–4196.
15. **Freeman-Cook, L. L., J. M. Sherman, C. B. Brachmann, R. C. Allshire, J. D. Boeke, and L. Pillus.** 1999. The Schizosaccharomyces pombe hst4(+) gene is a SIR2 homologue with silencing and centromeric functions. Mol. Biol. Cell **10:**3171–3186.
16. **Garcia-Sanchez, S., A. L. Mavor, C. L. Russell, S. Argimon, P. Dennison, B. Enjalbert, and A. J. Brown.** 2005. Global roles of Ssn6 in Tup1- and Nrg1-dependent gene regulation in the fungal pathogen, Candida albicans. Mol. Biol. Cell **16:**2913–2925.
17. **Grbavec, D., R. Lo, Y. Liu, A. Greenfield, and S. Stifani.** 1999. Groucho/transducin-like enhancer of split (TLE) family members interact with the yeast transcriptional co-repressor SSN6 and mammalian SSN6-related proteins: implications for evolutionary conservation of transcription repression mechanisms. Biochem. J. **337**(Pt 1):13–17.
18. **Greenall, A., A. P. Hadcroft, P. Malakasi, N. Jones, B. A. Morgan, C. S. Hoffman, and S. K. Whitehall.** 2002. Role of fission yeast Tup1-like repressors and Prr1 transcription factor in response to salt stress. Mol. Biol. Cell **13:**2977–2989.
19. **Herschbach, B. M., M. B. Arnaud, and A. D. Johnson.** 1994. Transcriptional repression directed by the yeast alpha 2 protein in vitro. Nature **370:**309–311.
20. **Huang, M., Z. Zhou, and S. J. Elledge.** 1998. The DNA replication and damage checkpoint pathways induce transcription by inhibition of the Crt1 repressor. Cell **94:**595–605.
21. **Hughes, T. R., M. J. Marton, A. R. Jones, C. J. Roberts, R. Stoughton, C. D. Armour, H. A. Bennett, E. Coffey, H. Dai, Y. D. He, M. J. Kidd, A. M. King, M. R. Meyer, D. Slade, P. Y. Lum, S. B. Stepaniants, D. D. Shoemaker, D. Gachotte, K. Chakraburtty, J. Simon, M. Bard, and S. H. Friend.** 2000. Functional discovery via a compendium of expression profiles. Cell **102:**109–126.
22. **Hwang, C. S., J. H. Oh, W. K. Huh, H. S. Yim, and S. O. Kang.** 2003. Ssn6, an important factor of morphological conversion and virulence in Candida albicans. Mol. Microbiol. **47:**1029–1043.
23. **Jabet, C., E. R. Sprague, A. P. VanDemark, and C. Wolberger.** 2000. Characterization of the N-terminal domain of the yeast transcriptional repressor Tup1. Proposal for an association model of the repressor complex Tup1 x Ssn6. J. Biol. Chem. **275:**9011–9018.
24. **Janoo, R. T., L. A. Neely, B. R. Braun, S. K. Whitehall, and C. S. Hoffman.** 2001. Transcriptional regulators of the Schizosaccharomyces pombe fbp1 gene include two redundant Tup1p-like corepressors and the CCAAT binding factor activation complex. Genetics **157:**1205–1215.
25. **Keleher, C. A., C. Goutte, and A. D. Johnson.** 1988. The yeast cell-type-specific repressor alpha 2 acts cooperatively with a non-cell-type-specific protein. Cell **53:**927–936.
26. **Keleher, C. A., M. J. Redd, J. Schultz, M. Carlson, and A. D. Johnson.** 1992. Ssn6-Tup1 is a general repressor of transcription in yeast. Cell **68:**709–719.
27. **Kim, S. J., M. J. Swanson, H. Qiu, C. K. Govind, and A. G. Hinnebusch.**

2005. Activator Gcn4p and Cyc8p/Tup1p are interdependent for promoter occupancy at ARG1 in vivo. Mol. Cell. Biol. **25:**11171–11183.
28. **Komachi, K., M. J. Redd, and A. D. Johnson.** 1994. The WD repeats of Tup1 interact with the homeo domain protein alpha 2. Genes Dev. **8:**2857–2867.
29. **Kuchin, S., and M. Carlson.** 1998. Functional relationships of Srb10-Srb11 kinase, carboxy-terminal domain kinase CTDK-I, and transcriptional corepressor Ssn6-Tup1. Mol. Cell. Biol. **18:**1163–1171.
30. **Lahn, B. T., and D. C. Page.** 1997. Functional coherence of the human Y chromosome. Science **278:**675–680.
31. **Lengronne, A., Y. Katou, S. Mori, S. Yokobayashi, G. P. Kelly, T. Itoh, Y. Watanabe, K. Shirahige, and F. Uhlmann.** 2004. Cohesin relocation from sites of chromosomal loading to places of convergent transcription. Nature **430:**573–578.
32. **Mukai, Y., E. Matsuo, S. Y. Roth, and S. Harashima.** 1999. Conservation of histone binding and transcriptional repressor functions in a *Schizosaccharomyces pombe* Tup1p homolog. Mol. Cell. Biol. **19:**8461–8468.
33. **Nehlin, J. O., M. Carlberg, and H. Ronne.** 1991. Control of yeast GAL genes by MIG1 repressor: a transcriptional cascade in the glucose response. EMBO J. **10:**3373–3377.
34. **Papamichos-Chronakis, M., R. S. Conlan, N. Gounalaki, T. Copf, and D. Tzamarias.** 2000. Hrs1/Med3 is a Cyc8-Tup1 corepressor target in the RNA polymerase II holoenzyme. J. Biol. Chem. **275:**8397–8403.
35. **Papamichos-Chronakis, M., T. Petrakis, E. Ktistaki, I. Topalidou, and D. Tzamarias.** 2002. Cti6, a PHD domain protein, bridges the Cyc8-Tup1 corepressor and the SAGA coactivator to overcome repression at GAL1. Mol. Cell **9:**1297–1305.
36. **Pickles, L. M., S. M. Roe, E. J. Hemingway, S. Stifani, and L. H. Pearl.** 2002. Crystal structure of the C-terminal WD40 repeat domain of the human Groucho/TLE1 transcriptional corepressor. Structure **10:**751–761.
37. **Proft, M., and K. Struhl.** 2002. Hog1 kinase converts the Sko1-Cyc8-Tup1 repressor complex into an activator that recruits SAGA and SWI/SNF in response to osmotic stress. Mol. Cell **9:**1307–1317.
38. **Redd, M. J., M. B. Arnaud, and A. D. Johnson.** 1997. A complex composed of tup1 and ssn6 represses transcription in vitro. J. Biol. Chem. **272:**11193–11197.
39. **Robyr, D., and M. Grunstein.** 2003. Genomewide histone acetylation microarrays. Methods **31:**83–89.
40. **Robyr, D., Y. Suka, I. Xenarios, S. K. Kurdistani, A. Wang, N. Suka, and M. Grunstein.** 2002. Microarray deacetylation maps determine genome-wide functions for yeast histone deacetylases. Cell **109:**437–446.
41. **Saito, J., T. Kon, A. Nagasaki, H. Adachi, and K. Sutoh.** 1998. Dictyostelium TRFA homologous to yeast Ssn6 is required for normal growth and early development. J. Biol. Chem. **273:**24654–24659.
42. **Sinha, I., M. Wiren, and K. Ekwall.** 2006. Genome-wide patterns of histone modifications in fission yeast. Chromosome Res. **14:**95–105.
43. **Smith, R. L., and A. D. Johnson.** 2000. Turning genes off by Ssn6-Tup1: a conserved system of transcriptional repression in eukaryotes. Trends Biochem. Sci. **25:**325–330.
44. **Smith, R. L., M. J. Redd, and A. D. Johnson.** 1995. The tetratricopeptide repeats of Ssn6 interact with the homeo domain of alpha 2. Genes Dev. **9:**2903–2910.
45. **Struhl, K., D. Kadosh, M. Keaveney, L. Kuras, and Z. Moqtaderi.** 1998. Activation and repression mechanisms in yeast. Cold Spring Harb. Symp. Quant. Biol. **63:**413–421.
46. **Tzamarias, D., and K. Struhl.** 1995. Distinct TPR motifs of Cyc8 are involved in recruiting the Cyc8-Tup1 corepressor complex to differentially regulated promoters. Genes Dev. **9:**821–831.
47. **Tzamarias, D., and K. Struhl.** 1994. Functional dissection of the yeast Cyc8-Tup1 transcriptional co-repressor complex. Nature **369:**758–761.
48. **Varanasi, U. S., M. Klis, P. B. Mikesell, and R. J. Trumbly.** 1996. The Cyc8 (Ssn6)-Tup1 corepressor complex is composed of one Cyc8 and four Tup1 subunits. Mol. Cell. Biol. **16:**6707–6714.
49. **Wang, A., S. K. Kurdistani, and M. Grunstein.** 2002. Requirement of Hos2 histone deacetylase for gene activity in yeast. Science **298:**1412–1414.
50. **Watson, A. D., D. G. Edmondson, J. R. Bone, Y. Mukai, Y. Yu, W. Du, D. J. Stillman, and S. Y. Roth.** 2000. Ssn6-Tup1 interacts with class I histone deacetylases required for repression. Genes Dev. **14:**2737–2744.
51. **Wiren, M., R. A. Silverstein, I. Sinha, J. Walfridsson, H. M. Lee, P. Laurenson, L. Pillus, D. Robyr, M. Grunstein, and K. Ekwall.** 2005. Genome-wide analysis of nucleosome density histone acetylation and HDAC function in fission yeast. EMBO J. **24:**2906–2918.
52. **Wu, J., N. Suka, M. Carlson, and M. Grunstein.** 2001. TUP1 utilizes histone H3/H2B-specific HDA1 deacetylase to repress gene activity in yeast. Mol. Cell **7:**117–126.
53. **Xue, Y., S. A. Haas, L. Brino, A. Gusnanto, M. Reimers, D. Talibi, M. Vingron, K. Ekwall, and A. P. H. Wright.** 2004. A DNA microarray for fission yeast: minimal changes in global gene expression after temperature shift. Yeast **21:**25–39.
54. **Zaman, Z., A. Z. Ansari, S. S. Koh, R. Young, and M. Ptashne.** 2001. Interaction of a transcriptional repressor with the RNA polymerase II holoenzyme plays a crucial role in repression. Proc. Natl. Acad. Sci. USA **98:**2550–2554.
55. **Zeeberg, B. R., W. Feng, G. Wang, M. D. Wang, A. T. Fojo, M. Sunshine, S. Narasimhan, D. W. Kane, W. C. Reinhold, S. Lababidi, K. J. Bussey, J. Riss, J. C. Barrett, and J. N. Weinstein.** 2003. GoMiner: a resource for biological interpretation of genomic and proteomic data. Genome Biol. **4:**R28.
56. **Zhang, Z., and J. C. Reese.** 2004. Redundant mechanisms are used by Ssn6-Tup1 in repressing chromosomal gene transcription in Saccharomyces cerevisiae. J. Biol. Chem. **279:**39240–39250.
57. **Zhang, Z., U. Varanasi, P. Carrico, and R. J. Trumbly.** 2002. Mutations of the WD repeats that compromise Tup1 repression function maintain structural integrity of the WD domain trypsin-resistant core. Arch. Biochem. Biophys. **406:**47–54.
58. **Zhu, X., M. Wiren, I. Sinha, N. N. Rasmussen, T. Linder, S. Holmberg, K. Ekwall, and C. M. Gustafsson.** 2006. Genome-wide occupancy profile of mediator and the Srb8-11 module reveals interactions with coding regions. Mol. Cell **22:**169–178.